

Speed Sensorless Model Predictive Current Control of Linear Induction Machines in Urban Transit

Samir A. Hamad^{1,*}, Ramadan M. Mostafa¹, Jean Thomas², E. G. Shehata³, Ahmed A. Zaki Diab^{3,**}

¹Process Control Technology Dept., Faculty of Technology and Education, Beni-Suef University, Beni-Suef, Egypt

²Electrical Engineering Dept., Faculty of Engineering, Beni-Suef University, Beni-Suef, Egypt

³Electrical Engineering Dept., Faculty of Engineering, Minia University, El Minia, Egypt

Corresponding authors: * samireng46@techedu.bsu.edu.eg and ** a.diab@mu.edu.eg

ARTICLE INFO

Article history:

Received:

Accepted:

Online:

Keywords:

Model predictive current control (MPCC)

Linear induction machine (LIM)

Weighting factor (WF)

ABSTRACT

There is an increasing interest in achieving global goals of mitigating climate changes that target environment protection. Thus, electric vehicles (as linear metros) were elaborated to avoid greenhouse gas emissions which negatively impact climate. Hence, in this paper, a finite control set-model predictive current control (FCS-MPCC) method of linear induction machine (LIM) was proposed for linear metro drives to achieve lower thrust ripples and eliminate selection of weighting factor (WF), the main limitation of conventional finite control set-model predictive thrust control (FCS-MPTC). Also, a model reference adaptive system (MRAS) was used for speed estimation due to some environmental considerations and cost-effectiveness. The proposed method used a single cost function that avoided the existence of WF and consisted of primary current errors between the predicted values and their references in $\alpha\beta$ -axes. A comparison between the FCS-MPTC and the suggested control method was conducted using Matlab/Simulink under a wide range of operating circumstances and via uncertainty validations issues, on the basis of one 3 kW arc induction machine (which constructed to imitate the actual behavior of the LIM). The extensive simulation results revealed that the proposed FCS-MPCC method can lead to much lower thrust ripples without heavy calculation steps. Moreover, the speed error between the estimated and actual speeds is about 0.025% of the reference value which validates the speed estimation scheme.

Nomenclature

| | |
|--------------------------------|---|
| LIM | Linear induction machine. |
| FCS-MPCC | Finite control set-model predictive current control. |
| FCS-MPTC | Finite control set-model predictive thrust control. |
| WF | Weighting factor. |
| MRAS | Model reference adaptive system. |
| ORIM | Ordinary rotating induction motor. |
| FOC | Field oriented control. |
| DTC | Direct thrust control. |
| DTC-SVM | DTC based on space vector modulation. |
| u_α and u_β | Voltages of the $\alpha\beta$ axes components. |
| i_α and i_β | Currents of the $\alpha\beta$ axes components. |
| ψ_α and ψ_β | flux linkages of the $\alpha\beta$ axes components. |
| subscripts p and s | Primary and secondary variables. |
| R | Resistances. |
| L | Mutual inductance. |
| L_D , L_{m0} and L_{ls} | Primary machine length, ordinary mutual inductance and secondary inductance at still. |
| L_{lp} | Primary inductance at standstill. |
| ω | Machine speed. |
| v_p | Machine linear speed. |
| F_l | Thrust load. |
| M | Mass. |
| D | Viscous coefficient. |
| J | COST function. |

1. Introduction

As a result of the growing interest in reaching global goals of climate change which aim to protect the environment, means of transportation based on electric motors (such as trains) have been widely used to eliminate greenhouse gas emissions, especially linear electric motors (LEMs). One of most attractive LEMs is Linear induction motor (LIM) has been emerged as a suitable candidate in various applications superior to ordinary rotating induction motor (ORIM) because of their merits of simple structure, strong acceleration or deceleration, direct linear motion, and low maintenance cost without mechanical transmission, and so on [1-3]. Despite the abovementioned merits of LIMs, due to large air-gap length and the straight magnetic circuits (cut-open magnetic circuit of the primary), they have some limitations which deteriorate the drive performance. This special structure of the LIMs leads to effects with both ends (entry end and exit end); this end effect causes variable mutual inductance as the machine speed increases [4]. Therefore, the control characteristics of LIMs are more sophisticated than those of ORIMs due to ignoring the influence of the end effects by classical control techniques [5].

These limitations associated with the conventional LIMs control techniques can be overcome by establishing convenient and robust control strategies. Direct thrust control (DTC) was suggested to attain fast dynamic thrust response and to overcome some demerits like machine parameters, coordinate transformation and controls loop required in field oriented control (FOC), making DTC less complicated than FOC. Away from the merits of DTC, because it is based on hysteresis controllers and an offline switching table it has some problems which are inevitable as variable switching frequency and tremendous

fluctuations for both thrust and flux, which would cause imperfect control performance [6]. DTC based on space vector modulation (DTC-SVM) method is employed in [7] to reduce the higher ripples but is insufficient to achieve constant switching frequency.

In most recently, finite control set-model predictive thrust control (FCS-MPTC) has been admitted as the most convenient control approach in various power electronics applications and many machine drive systems [8]. FCS-MPTC is an attempt to combine model predictive control and DTC due to the discrete nature of power converters and the limited number of switching cases of the major two-level three-phase inverter [9]. FCS-MPTC has become the most suitable control option to prior control techniques, owing to multivariable control, simplicity, and online

$$F_e = (3\pi / 2\tau)(\psi_{\alpha p} i_{\beta p} - \psi_{\beta p} i_{\alpha p}) \quad (6)$$

evaluation to pick out the most appropriate switching vector that offers the minimum cost function value [10]. Both errors between thrust and flux predicted values and their references are routinely included in the FCS-MPTC cost function for LIMs drive control systems [11]. As a result, the weighting factor (WF) must exist in order to balance the non-unifying dimensions and give a higher priority to on term than to the other.

To date, empirical methods and tremendous effort have been employed to obtain a suitable WF, which is a significantly more challenging and complex undertaking [12]. Consequently, a variety of approaches are suggested to address this problem while avoiding the usage of WF [13, 14].

Therefore, to avoid the WF's time-consuming procedures and calculations, this paper presents a finite control set-model predictive control (FCS-MPCC) method, which can lessen the calculation burden, eliminate the use of the WF in the cost function, and furthermore present lower thrust fluctuations compared to those of the conventional FCS-MPTC. Also, the model reference adaptive system (MRAS) was used for speed estimation due to some environmental considerations and also for being cost-effective.

2. Modeling and Analysis of the LIM

The LIM equivalent circuit for some extent will be identical to that of ORIMs without considering the influence of end effects. Depending on the suggested LIM equivalent circuit in [15], the model of LIM in the stationary frame, which takes a full consideration of the influence of the end effect, can be further modified as follows [16]:

$$\frac{di_{\alpha p}}{dt} = \frac{1}{\sigma} \left[u_{\alpha p} - \left(R_p + \frac{L_m}{T_r T_l} \right) i_{\alpha p} + \frac{1}{T_l} \left(\frac{\psi_{\alpha s}}{T_r} + \omega_s \psi_{\beta s} \right) \right] \quad (1)$$

$$\frac{di_{\beta p}}{dt} = \frac{1}{\sigma} \left[u_{\beta p} - \left(R_p + \frac{L}{T_r T_l} \right) i_{\beta p} + \frac{1}{T_l} \left(\frac{\psi_{\beta s}}{T_r} - \omega_s \psi_{\alpha s} \right) \right] \quad (2)$$

$$\frac{d\psi_{\alpha s}}{dt} = \frac{1}{T_r} (L_m i_{\alpha p} - \psi_{\alpha s} - T_r \omega_s \psi_{\beta s}) \quad (3)$$

$$\frac{d\psi_{\beta s}}{dt} = \frac{1}{T_r} (L_m i_{\beta p} - \psi_{\beta s} + T_r \omega_s \psi_{\alpha s}) \quad (4)$$

In the aforementioned equations, u_α and u_β , i_α and i_β , and ψ_α and ψ_β are voltages, currents, and flux linkages of the α - β axes components, respectively. The subscripts p and s refer to primary and secondary variables, respectively. The resistances, machine speed and mutual inductance of the LIM are represented by R , L , ω and L_m , respectively, $\sigma = (L_p L_s - L_m^2) / L_s$, $T_r = L_s / R_s$, and $T_l = L_s / L_m$.

The load equation is determined as

$$F_e = M p v_p + D v_p + F_l \quad (5)$$

where F_l is the thrust load, the viscous coefficient is D , the mass is M , and the machine linear speed is v_p . Also, the thrust can be expressed by the primary current and flux, as illustrated by

Some LIM parameters would be modified after considering the end-effect influence on the LIM parameters as mutual inductance, which depends on the value of $f(Q)$ that expresses the average attenuation rate of the flux related to the end-effect coefficient, as given by

$$f(Q) = [1 - \exp(-Q)] / Q \quad (7)$$

$$Q = L_D R_s / [(L_{m0} + L_{ls}) v_p] \quad (8)$$

$$L_m = [1 - f(Q)] L_{m0} \quad (9)$$

where L_D , L_{m0} and L_{ls} are primary machine length, ordinary mutual inductance and secondary inductance at still. Moreover, in turn, it leads to the modification of the primary and secondary inductances as given by

$$L_p = L_{ip} + L_m \quad (10)$$

$$L_s = L_{ls} + L_m \quad (11)$$

where L_{ip} is the primary inductance at standstill.

3. Proposed Strategies of the LIM

This section presented briefly two methods of finite control set-model predictive control and consequently, explains the main implementation steps of each method individually.

1.1. FCS-MPTC for LIM

The FCS-MPTC is proposed as an alternative method to the DTC, aiming to mitigate the high fluctuation of thrust associated with the DTC method. FCS-MPTC strategy usually includes three main steps, which can be briefly expressed as follows:

- Step 1: Both secondary and primary fluxes are estimated based on the flux observer, which is presented in [17] as follows:

$$\psi_{\alpha p}^{(k)} = T_s u_{\alpha p}^{(k)} - T_s R_p i_{\alpha p}^{(k)} + \psi_{\alpha p}^{(k-1)} \quad (12)$$

$$\psi_{\beta p}^{(k)} = T_s u_{\beta p}^{(k)} - T_s R_p i_{\beta p}^{(k)} + \psi_{\beta p}^{(k-1)} \quad (13)$$

$$\psi_{\alpha s}^{(k)} = T_l \psi_{\alpha p}^{(k)} + \left(L_m - \frac{L_p L_s}{L_m} \right) i_{\alpha p}^{(k)} \quad (14)$$

$$p\psi_{\alpha s}^* = T_l \left(u_{\alpha p} - (R_p + L_p \sigma p) i_{\alpha p} \right) \quad (22)$$

$$p\psi_{\beta s}^* = T_l \left(u_{\beta p} - (R_p + L_p \sigma p) i_{\beta p} \right) \quad (23)$$

$$\psi_{\beta s}^{(k)} = T_l \psi_{\beta p}^{(k)} + \left(L_m - \frac{L_p L_s}{L_m} \right) i_{\beta p}^{(k)} \quad (15)$$

- Step 2: Primary flux, primary current and thrust are predicted based on Euler's first-order formula for the control instant by the following equations:

$$\psi_{\alpha p}(k+1) = T_s u_{\alpha p}(k) - T_s R_p i_{\alpha p}(k) + \psi_{\alpha p}(k) \quad (16)$$

$$\psi_{\beta p}(k+1) = T_s u_{\beta p}(k) - T_s R_p i_{\beta p}(k) + \psi_{\beta p}(k) \quad (17)$$

$$i_{\alpha p}(k+1) = \left(1 - \frac{T_s}{\sigma} \left(R_p + \frac{R_s}{T_l^2} \right) \right) i_{\alpha p}(k) + \frac{T_s}{\sigma} \left(u_{\alpha p}(k) + \frac{1}{T_l T_r} (\psi_{\alpha s}(k) + T_r \omega_s \psi_{\beta s}(k)) \right) \quad (18)$$

$$i_{\beta p}(k+1) = \left(1 - \frac{T_s}{\sigma} \left(R_p + \frac{R_s}{T_l^2} \right) \right) i_{\beta p}(k) + \frac{T_s}{\sigma} \left(u_{\beta p}(k) + \frac{1}{T_l T_r} (\psi_{\beta s}(k) - T_r \omega_s \psi_{\alpha s}(k)) \right) \quad (19)$$

$$J = (F_e^* - F_e(k+1))^2 + F(\psi_p^* - \psi_p(k+1))^2 \quad (21)$$

$$F_e(k+1) = (3\pi/2\tau) (\psi_{\alpha p}(k+1) i_{\beta p}(k+1) - \psi_{\beta p}(k+1) i_{\alpha p}(k+1)) \quad (20)$$

- Step 3: Optimization of the cost function, which comprised of the errors between the predicted thrust and primary flux with their references values. In FCS-MPTC, the cost function, J, is formulated by

1.2. Speed Estimation for LIM Based on Model Reference Adaptive System

Instead of using a mechanical encoder to detect the speed signal, due to maintenance requirements, mechanical arrangements, as well as the overall system's high cost, which would be a disadvantage for the control system, speed estimation may be implemented. To improve the control system's reliability while lowering the overall cost, a speed estimation method is preferred to attain a reliable and stable driving system [18]. So, variety of sensorless schemes for speed estimation are used like speed adaptive based flux observer (Leunberger's observer) [19], sliding mode observer (SMO) [20], and extended Kalman filter [21] as well as model reference adaptive systems [22]. From the

preceding methods for estimating the speed, MRAS is a straightforward and easy for implementation [24].

The estimated speed in the MRAS observer can be calculated using the error of back electromagnetic force, the error of active power, the error of reactive power and the error of induced flux [23]. The MRAS observer's principle is built on two models named the adjustable model and the reference model with an adaption mechanism to attain the estimated speed. The block diagram of MRAS structure is shown in Figure 1. The detailed structure of MRAS can be represented in the following stages.

- The reference model (voltage model), is designed based on the primary voltage and does not include speed quantity, can be expressed as:
- The adjustable model (current model). In contrast to the reference model, the adjustable model bears the estimation parameters that can be represented as:

$$p\hat{\psi}_{\alpha s} = \frac{1}{T_r} \left(-\hat{\psi}_{\alpha s} - T_r \omega_s \hat{\psi}_{\beta s} + L_m i_{\alpha p} \right) \quad (24)$$

$$p\hat{\psi}_{\beta s} = \frac{1}{T_r} \left(-\hat{\psi}_{\beta s} + T_r \omega_s \hat{\psi}_{\alpha s} + L_m i_{\beta p} \right) \quad (25)$$

The adaptive mechanism is driven based on an error (the difference between the outputs of the two models) which is used as input of the PI controller.

- Thus, the error term between the outputs of the two models is

$$\varepsilon_r = (\hat{\psi}_{\alpha s} \psi_{\beta s}^* - \hat{\psi}_{\beta s} \psi_{\alpha s}^*) \quad (26)$$

Popov's hyperstability theory guides the choice of the rotor speed estimation algorithm (adaptation mechanism) [24]. The PI controllers can be employed as adaptation mechanisms, to regulate the estimated speed and to adjust the estimated secondary flux to its reference value.

1.3. Proposed FCS-MPCC Without WF

To date, there is a scarcity of accurate approaches that explain how to select the best appropriate WF without arduous tweaking work. Consequently, an FCS-MPCC is presented, which tries to keep the $\alpha\beta$ -axes currents as close as feasible to the reference currents. In the FCS-MPCC, there are usually three stages (estimation, prediction, and cost function evaluation), which can be elaborated as follows.

- 1) The estimation of the secondary flux: Depending on the presented flux representations in [25], the estimation of the secondary flux can be obtained as

$$\psi_{\alpha s}(k) = \left[\frac{T_s R_s L_m \times i_{\alpha p}(k)}{T_s R_s + L_s} \right] + \left[\frac{L_s \psi_{\alpha s}(k-1) - T_s L_s \omega_s \psi_{\beta s}(k)}{T_s R_s + L_s} \right] \quad (27)$$

$$\psi_{\beta s}(k) = \left[\frac{T_s R_s L_m \times i_{\beta p}(k)}{T_s R_s + L_s} \right] + \left[\frac{L_s \psi_{\beta s}(k-1) + T_s L_s \omega_s \psi_{\alpha s}(k)}{T_s R_s + L_s} \right] \quad (28)$$

- 2) Prediction of the primary current for the next-instant: on the basis of Euler's first-order formula, the $\alpha\beta$ -axes primary currents of the next control period are predicted as

$$i_{\alpha p}(k+1) = \left[i_{\alpha p}(k) \times \left[1 - \left(\frac{T_s}{\sigma} \right) \left(R_p + \frac{R_s L_m}{T_l} \right) \right] \right] + \frac{T_s}{\sigma} \times \left[\frac{1}{T_l T_r} (\psi_{\alpha s} + T_r \omega_s \psi_{\beta s}) + u_{\alpha p}(k) \right] \quad (29)$$

$$i_{\beta p}(k+1) = \left[i_{\beta p}(k) \times \left[1 - \left(\frac{T_s}{\sigma} \right) \left(R_p + \frac{R_s L_m}{T_l} \right) \right] \right] + \frac{T_s}{\sigma} \times \left[\frac{1}{T_l T_r} (\psi_{\beta s} - T_r \omega_s \psi_{\alpha s}) + u_{\beta p}(k) \right] \quad (30)$$

- 3) Design of FCS-MPCC cost function: The proposed FCS-MPCC method aims to have the $\alpha\beta$ -axes primary currents close to their reference values. Therefore, the most appropriate voltage vector minimizing the value of the cost function, J , makes the $\alpha\beta$ -axes primary currents track their desired values. Thus, the cost function can be expressed as follows

$$J = \left| i_{\alpha p}^* - i_{\alpha p}^{(k+1)} \right| + \left| i_{\beta p}^* - i_{\beta p}^{(k+1)} \right| \quad (31)$$

The block diagram of the proposed method with model reference adaptive system for speed estimation for LIM is shown in Figure 2.

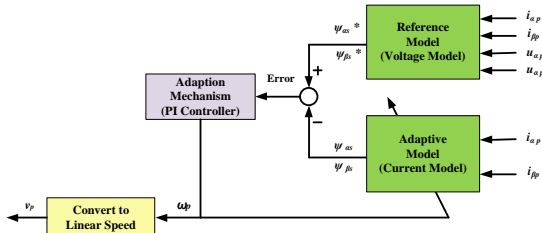


Figure 1: Basic Structure of Linear Speed Estimation Based MRAS.

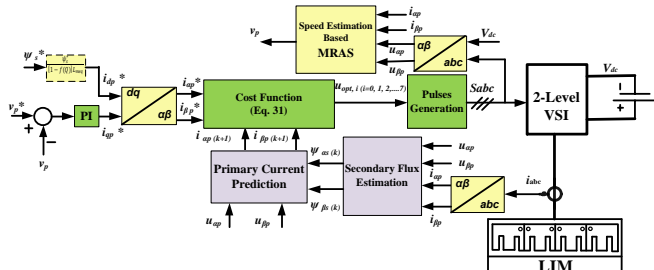


Figure 2: Control Diagram Based on the Proposed FCS-MPCC method for LIM

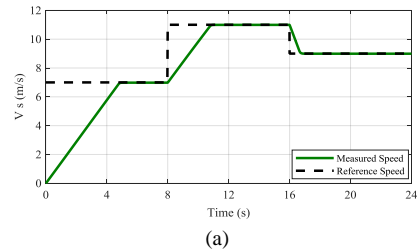
LIM.

4. Simulation and Discussions

In order to examine the effectiveness and the capability of the proposed FCS-MPCC based on speed sensorless is verified under two different operating circumstances and via uncertainty validations issues, a full comparison between the proposed method and the FCS-MPTC method is presented and discussed. The simulation has been conducted using the MATLAB/Simulink environment based on the 3kW nominal power of an arc induction motor with a large rotor radius equal to 1.25 m (simulation on the practical LIM). The main parameters of the system specification are listed in the Table 1.

1) Reference Speed Alteration

This case is presented to evaluate the control performance under three different reference speeds and a constant thrust load of 100 N. The reference speed is increased from 7 to 11 ms⁻¹ after time, t=8 s, and then it is decreased to 9 ms⁻¹ at time, t=16 s as shown in Figures 3 (a) and 4 (a). It is noticed from the linear speed profile that the actual linear speed response for both strategies follows the reference value gradually with a fast response. Furthermore, the speed estimation based on MRAS demonstrates that the linear speed can be determined without using any sensors, as shown in Figure 4 (a). In addition, the speed error between the measured speed and the estimated speed is depicted in Figure 4 (d), it can be observed that the error is small at a sudden increase of the reference speed but suffers from a slight drop at a sudden decreasing of the reference speed. The difference in linear speed between the measured and estimated speeds is roughly less than 0.02 ms⁻¹ (i.e. 0.025% of the reference speed) at the steady-state process, which proves the capability of the proposed MRAS in tracking the reference speed very well. On the other hand, Figure 3 (b) and Figure 4 (b) show the thrust profile of the FCS-MPTC and FCS-MPCC respectively. It can be observed that the proposed FCS-MPCC method can get lower ripples in response to those of the conventional method. Moreover, from the response of the three-phase currents based on the FCS-MPTC method as shown in Figure 3 (c) and the proposed method as shown in Figure 4 (c), the three-phase currents for both at the steady-state can be maintained at their reference levels. Finally, in order to clarify the superiority of the proposed FCS-MPCC method over the conventional one, Figure 5 displays the developed thrust by the two methods, demonstrating the effectiveness of the proposed method in reducing the thrust ripples.



(a)

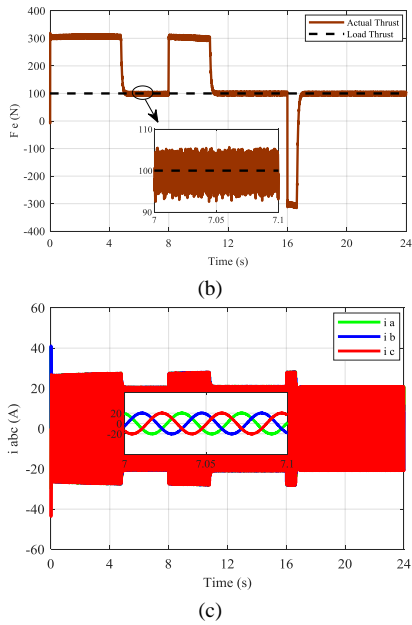


Figure 3: FCS-MPTC under variable speed. (a) Speed. (b) Thrust. (c) Three-phase current.

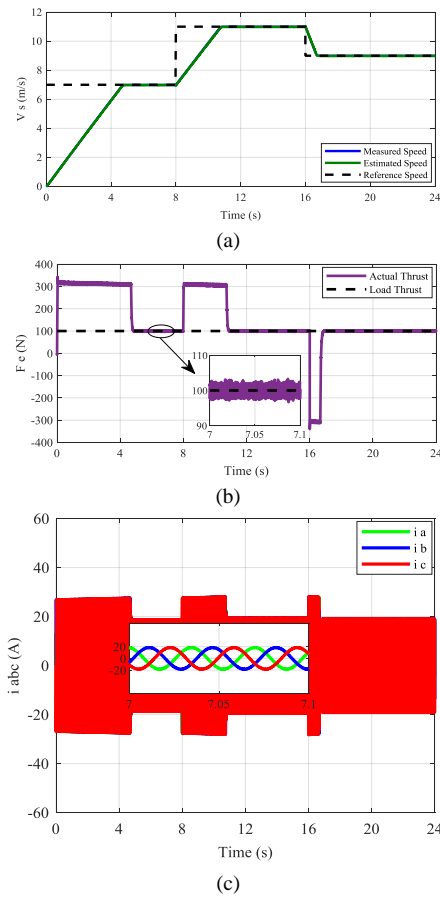


Figure 4: FCS-MPCC based MRAS under variable speed. (a) Speed. (b) Thrust. (c) Three-phase current, (d) speed error between the measured speed and the estimated speed.

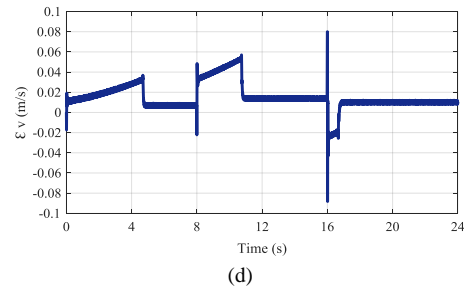


Figure 4: FCS-MPCC based MRAS under variable speed. (a) Speed. (b) Thrust. (c) Three-phase current, (d) speed error between the measured speed and the estimated speed.

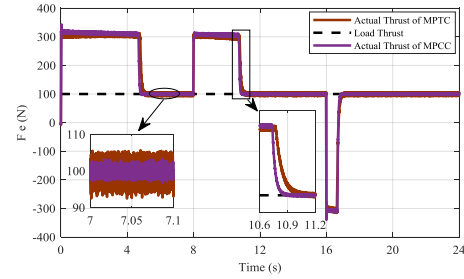


Figure 5: Thrust for both control methods at variable linear speeds.

2) Thrust Load Alteration

This subsection is presented to evaluate the drive performance under two different thrust loads and a constant linear speed of 8 ms^{-1} . The machine is loaded with a starting load of 120 N and after time, $t=12 \text{ s}$, the load is changed to 200 N. The profile of the linear speed response for the FCS-MPTC method and the proposed method based on the MRAS speed estimation method is shown in Figure 6 (a) and Figure 7 (a), respectively. It can be observed that, the actual speed tracks the desired speed with a fast response. Furthermore, the speed estimation based on MRAS demonstrates that the linear speed can be determined without using any sensors, as shown in Figure 7 (a). In addition, the speed error between the measured speed and the estimated speed is depicted in Figure 7 (d). It can be observed that, the error is very small (about 0.02 ms^{-1}); as 0.025% of the reference speed, which proves the capability of the proposed MRAS in tracking the reference speed very well. On the other hand, Figure 6 (b) and Figure 7 (b) show the thrust profile of the FCS-MPTC and FCS-MPCC methods, respectively. It can be observed that, the proposed FCS-MPCC method can get much lower ripples in response to those of the conventional method. Also, from the response of the three-phase currents based on the FCS-MPTC method as shown in Figure 6 (c) and the proposed method as shown in Figure 7 (c), at the steady state the three phase currents for both methods can be maintained at their reference levels. Lastly, in order to clarify the superiority of the proposed FCS-MPCC method over the conventional one, Figure 8 displays the developed thrust by the two methods, demonstrating that the proposed method succeeds in decreasing the thrust ripples.

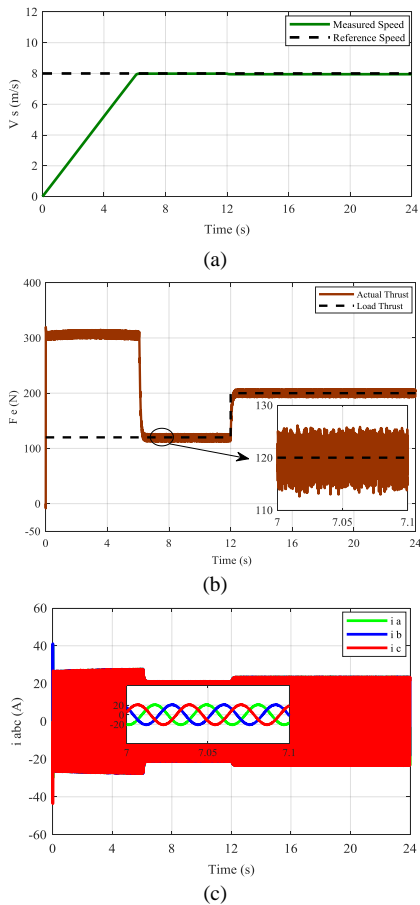


Figure 6: FCS-MPTC under variable load. (a) Speed. (b) Thrust. (c) Three-phase current.

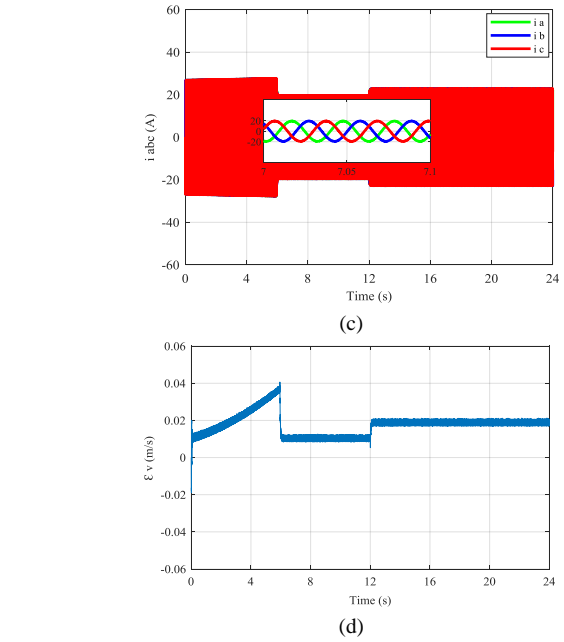
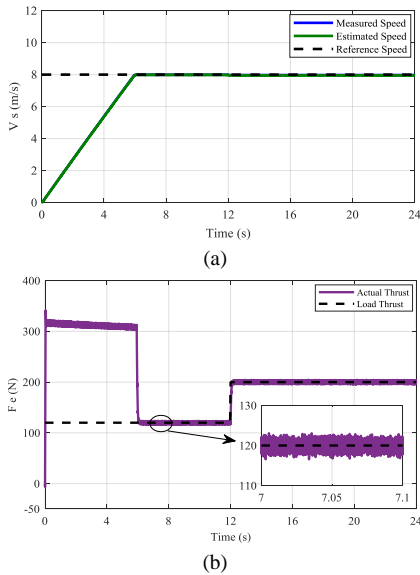


Figure 7: FCS-MPCC based on MRAS under variable load. (a) Speed. (b) Thrust. (c) Three-phase current, (d) speed error between the measured speed and the estimated speed.

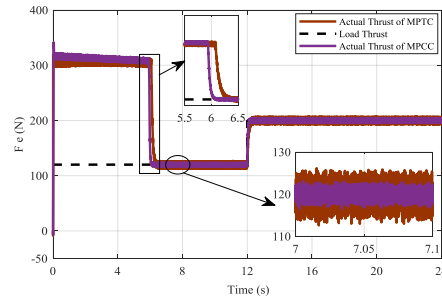
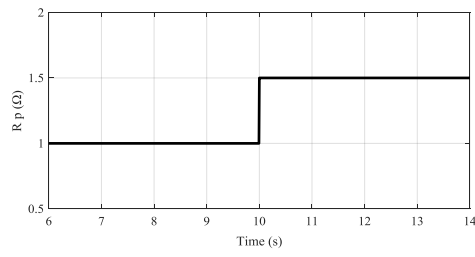


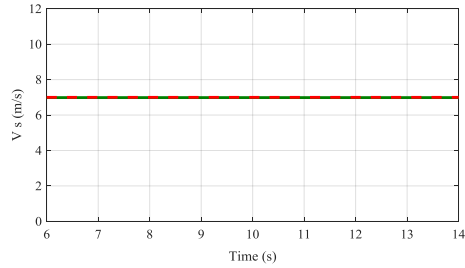
Figure 8: Thrust for both control methods at variable loads.

3) Parameters Uncertainty

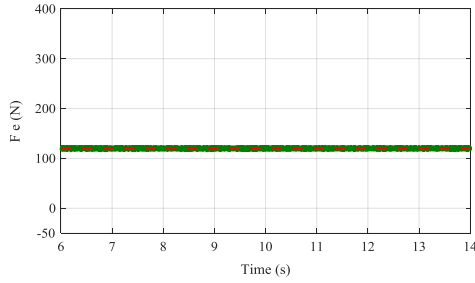
The proposed method is checked by parameters sensitivity analysis, to illustrate the effect of the parameters uncertainty on the system performance. Uncertainties in primary and secondary resistances and mutual inductance are examined by assuming a change of 150 % from their original values, to illustrate the influence of these mismatches on the proposed FCS-MPCC method. Therefore, a specific scenario is chosen to verify the impact of aforementioned parameters uncertainties, where the linear speed is 7 ms^{-1} and the load is fixed at 120 N during all cases. From Figure 9, Figure 10 and Figure 11, the impacts of mismatches on R_p , R_s , and L_{m0} are depicted, respectively. These Figures show that mismatches in both primary and secondary resistances do not affect the speed, thrust, and primary current. On the other hand, the mismatch of the mutual inductance has a minor effect on the thrust. So, the proposed FCS-MPCC method is slightly sensitive to the mutual inductance mismatch, but more robust in response to the mismatch of primary and secondary resistances.



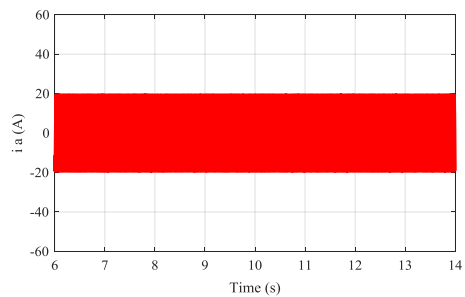
(a)



(b)

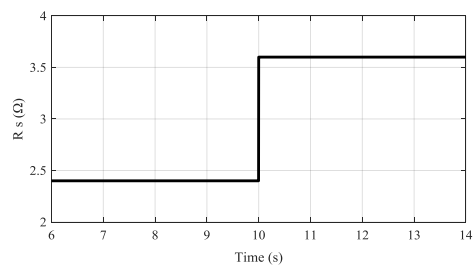


(c)

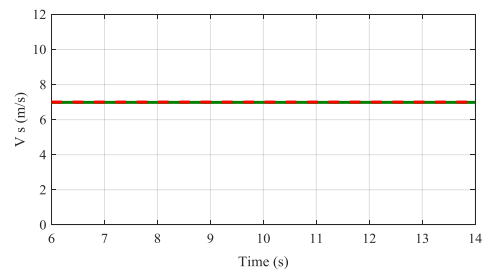


(d)

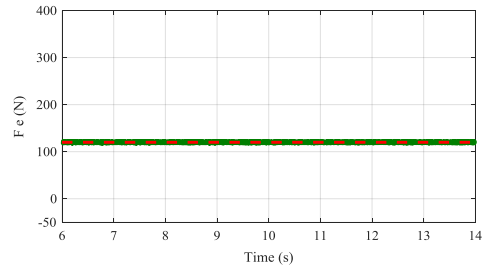
Figure 9: Influence of R_p mismatch on the proposed FCS-MPCC. (a) R_p . (b) Speed. (c) Thrust (d) A-phase current.



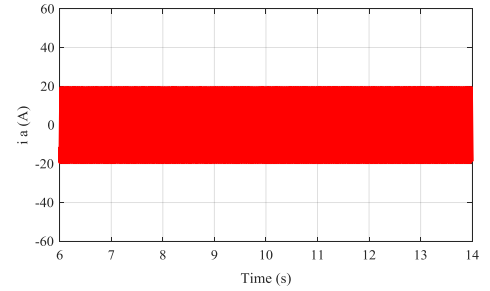
(a)



(b)

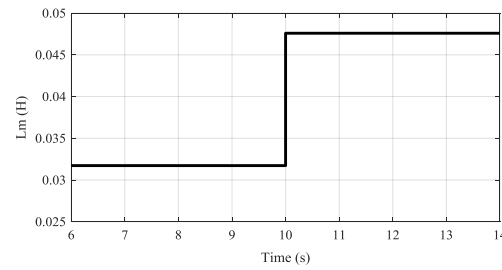


(c)

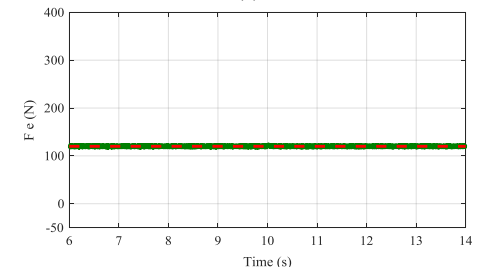


(d)

Figure 10: Influence of R_s mismatch on the proposed FCS-MPCC. (a) R_s . (b) Speed. (c) Thrust (d) A-phase current.



(a)



(b)

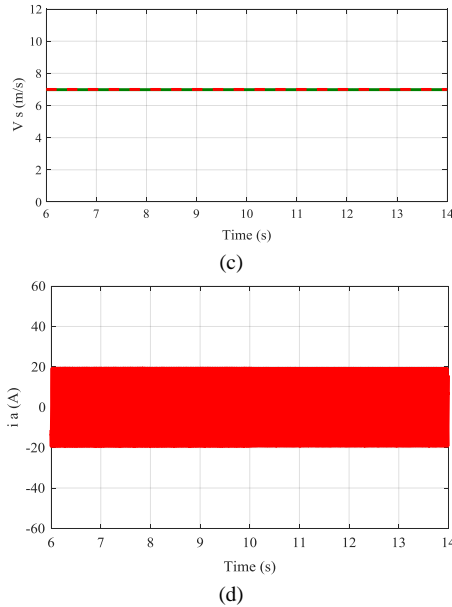


Figure 11: Influence of L_m mismatch on the proposed FCS-MPCC. (a) L_m . (b) Speed. (c) Thrust (d) A-phase current.

5. Conclusions

In this paper, to improve the overall performance of the LIM drive system, a strategy with the combination of FCS-MPCC and MRAS has been presented for LIM drive system. The proposed FCS-MPCC has been used to avoid the time-consuming task of determining an acceptable WF to balance the different units of the cost function terms with the conventional FCS-MPTC. The $\alpha\beta$ -axes components of both the reference and predicted primary current have been included in the presented cost function. The performance of the LIM drive system under the suggested FCS-MPCC strategy has been totally compared to that of the traditional FCS-MPTC strategy. Through the simulation validations, it has been evident that the proposed FCS-MPCC method can offer much lower thrust ripples compared to the conventional method. Moreover, based on the presented MRAS speed estimation the error between the estimated and measured speeds is 0.025% of the reference speed, which proves the capability and the effectiveness of the proposed method. In the future work, the validations of the suggested scheme should be achieved through the experimental tests.

Table 1: Specifications and Main Parameters of LIM

| LIM | |
|-----------------------------------|----------------------|
| Rated speed | $v_R = 11ms^{-1}$ |
| Rated current | $I_R = 22 A$ |
| Rated power | $P_R = 3 Kw$ |
| Rated thrust | $F_R = 280 N$ |
| Secondary resistance | $R_s = 2.4 \Omega$ |
| Primary length | $L_D = 1.3087 m$ |
| Primary resistance | $R_p = 1 \Omega$ |
| Mutual inductance (at standstill) | $L_{m0} = 31.725 mH$ |
| Pole pitch length | $\tau = 0.1485 m$ |
| Secondary leakage inductance | $L_{ls} = 4.3 mH$ |

References

- [1] I. Boldea, L. N. Tutelea, W. Xu and M. Pucci, "Linear electric machines, drives, and MAGLEVs: an overview," IEEE Trans. Ind. Electron., vol. 65, no. 9, pp. 7504-7515, Sept. 2018, doi: 10.1109/TIE.2017.2733492.
- [2] M. M. Ali, W. Xu, A. K. Junejo, M. F. Elmorshedy and Y. Tang, "One new super-twisting sliding mode direct thrust control for linear induction machine based on linear metro," IEEE Trans. Power Electron., vol. 37, no. 1, pp. 795-805, Jan. 2022, doi: 10.1109/TPEL.2021.3096066.
- [3] D. Hu, W. Xu, R. Dian and Y. Liu, "Loss minimization control strategy for linear induction machine in urban transit considering normal force," IEEE Trans. Ind. Appl., vol. 55, no. 2, pp. 1536-1549, Mar. 2019, doi: 10.1109/TIA.2018.2873575.
- [4] F. Alonge, M. Cirrincione, M. Pucci, and A. Sferlazza, "Input-output feedback linearization control with on-line MRAS-based inductor resistance estimation of linear induction motors including the dynamic end effects," IEEE Trans. Ind. Appl., vol. 52, no. 1, pp. 254-266, Jan. 2016, doi: 10.1109/TIA.2015.2465939.
- [5] M. A. Usta, O. Akyazi and A. S. Akpinar, "Simulation of direct thrust control for linear induction motor including end-effect," Int. Sym. Innovations in Intelligent Systems and Applications, 2012, pp. 1-5, doi: 10.1109/INISTA.2012.6246998.
- [6] H. Karimi, S. Vaez-Zadeh and F. Rajaei Salmasi, "Combined vector and direct thrust control of linear induction motors with end effect compensation," IEEE Trans. Ener. Conv., vol. 31, no. 1, pp. 196-205, Mar. 2016, doi: 10.1109/TEC.2015.2479251.
- [7] K. Wang, Y. Li, L. Shi and Q. Ge, "A novel switching scheme for direct thrust control of LIM with reduction of thrust ripple," Proc. Int. Con. Elect. Mach. Syst., 2010, pp. 1491-1494.
- [8] W. Xie, Xiaocan Wang, Fengxiang Wang, Wei Xu, Ralph M. Kennel, Dieter Gerling and Robert D. Lorenz, "Finite-control-set model predictive torque control with a deadbeat solution for PMSM drives," IEEE Trans. Ind. Electron., vol. 62, no. 9, pp. 5402-5410, Sept. 2015, doi: 10.1109/TIE.2015.2410767.
- [9] O. Sandre-Hernandez, J. Rangel-Magdaleno and R. Morales-Caporal, "A comparison on finite-set model predictive torque control schemes for PMSMs," IEEE Trans. Power Electron., vol. 33, no. 10, pp. 8838-8847, Oct. 2018, doi: 10.1109/TPEL.2017.2777973.
- [10] J. Rodriguez, Marian P. Kazmierkowski, Jose R. Espinoza, Pericle Zanchetta, Haitham Abu-Rub, Hector A. Young and Christian A. Rojas., "State of the art of finite control set model predictive control in power electronics," IEEE Trans. Ind. Infor., vol. 9, no. 2, pp. 1003-1016, May 2013, doi: 10.1109/TII.2012.2221469.
- [11] W. Xu, M. F. Elmorshedy, Y. Liu, M. R. Islam and S. M. Allam, "Finite-set model predictive control based thrust maximization of linear induction motors used in linear metros," in IEEE Trans. Veh. Technol., vol. 68, no. 6, pp. 5443-5458, June 2019, doi: 10.1109/TVT.2019.2909785.
- [12] F. Wang, H. Xie, Q. Chen, S. A. Davari, J. Rodríguez and R. Kennel, "Parallel predictive torque control for induction machines without weighting factors," in IEEE Trans. Power Electron., vol. 35, no. 2, pp. 1779-1788, Feb. 2020, doi: 10.1109/TPEL.2019.2922312.
- [13] S. A. Hamad, W. Xu, M. F. Elmorshedy and M. M. Ali, "Improved model predictive flux control of linear induction machine applied for linear metro," pro. Int. Con. Electrical Machines and Systems (ICEMS), 2020, pp. 1280-1285, doi: 10.23919/ICEMS50442.2020.9291209.
- [14] S. A. Hamad, W. Xu, A. Diab, M. M. Ali and S. A. Bukhari, "Model predictive voltage control for linear induction machine without weighting factor," pro. Int. Sym. on Lin. Drives Ind. App. (LDIA), 2021, pp. 1-6, doi: 10.1109/LDIA49489.2021.9506003.

- [15] J. Duncan "Linear induction motor-equivalent-circuit model," Proc. Inst. Elect. Eng., vol. 130, no. 1, pp. 51-57, Jan. 1983.
- [16] W. Xu, R. Islam, and M. Pucci, *Advanced linear machines and drive systems*, Springer-Verlag Berlin Heidelberg, Aug. 2019.
- [17] J. Zou, W. Xu, J. Zhu, and Y. Liu, "Low-complexity finite control set model predictive control with current limit for linear induction machines," *IEEE Trans. Ind. Electron.*, vol. 65, no. 12, pp. 9243–9254, Dec. 2018, doi: 10.1109/TIE.2018.2807369 .
- [18] Y. Liu, W. Xu, T. Long and F. Blaabjerg, "An improved rotor speed observer for standalone brushless doubly-fed induction generator under unbalanced and nonlinear loads," *IEEE Trans. Power Electron.*, vol. 35, no. 1, pp. 775-788, Jan. 2020, doi: 10.1109/TPEL.2019.2915360.
- [19] H. Kubota, K. Matsuse and T. Nakano, "DSP-based speed adaptive flux observer of induction motor," *IEEE Trans. Ind. Appl.*, vol. 29, no. 2, pp. 344-348, March-April 1993, doi: 10.1109/28.216542.
- [20] Masoumi Kazraji, Saeed, Soflayi, Ramin and Bannae Sharifian, Mohammad Bagher. "Sliding-mode observer for speed and position sensorless control of linear-PMSM," *Electrical, Control and Communication Engineering*, May. 2014, doi: 5. 10.2478/ecce-2014-0003.
- [21] M. Habibullah and D. D. Lu, "A speed-sensorless FS-PTC of induction motors using extended kalman filters," *IEEE Trans. Ind. Electron.*, vol. 62, no. 11, pp. 6765-6778, Nov. 2015, doi: 10.1109/TIE.2015.2442525.
- [22] M. A. Mossa and S. Bolognani, "Effective model predictive current control for a sensorless IM drive," *IEEE Int. Sym. Sensorless Control for Electrical Drives (SLED)*, 2017, pp. 37-42, doi: 10.1109/SLED.2017.8078427.
- [23] R. Kumar, S. Das, P. Syam and A. K. Chattopadhyay, "Review on model reference adaptive system for sensorless vector control of induction motor drives," *IET Elect. Power Appl.*, vol. 9, no. 7, pp. 496-511, Feb. 2015, doi: 10.1049/iet-epa.2014.0220.
- [24] M. F. Elmorshedy, W. Xu, M. M. Ali, Y. Liu and S. M. Allam, "High Performance Speed Sensorless Finite-Set Predictive Thrust Control of a Linear Induction Motor based on MRAS and Fuzzy Logic Controller," *2020 IEEE 9th International Power Electronics and Motion Control Conference (IPEMC2020-ECCE Asia)*, 2020, pp. 3039-3044, doi: 10.1109/IPEMC-ECCEAsia48364.2020.9367640.
- [25] W. Xu, M. F. Elmorshedy, Y. Liu, J. Rodriguez and C. Garcia, "Maximum thrust per ampere of linear induction machine based on finite-set model predictive direct thrust control," *IEEE Trans. Power Electron.*, vol. 35, no. 7, pp. 7366-7378, July 2020, doi: 10.1109/TPEL.2019.2960280.